A Quantitative Structure−Property Relationship Study of the Glass Transition Temperature of OLED Materials

ShiWei Yin,[†] Z. Shuai,*,[†] and Yilin Wang[‡]

Laboratory of Organic Solids, Center for Molecular Sciences, Institute of Chemistry, The Chinese Academy of Sciences, Beijing 100080, P. R. China and Laboratory of Colloid and Interface Sciences, Institute of Chemistry, The Chinese Academy of Sciences, Beijing 100080, P. R. China

Organic light-emitting-diodes (OLED) materials possess great potential applications. Stability and efficiency are the two major factors to be improved toward commercialization, especially the thermal stability, because in the working device, the organic molecular materials can have high temperature. One of the most important factors, which influences the stability, is the glass transition temperature (T_g). We employed a QSPR (quantitative structure-properties relationship) approach to establish a theoretical model to predict the glass transition temperatures of organic molecular materials. A six-parameter correlation with the squared correlation coefficient $R^2 = 0.9270$ and the average absolute error 8.5 K was developed for a diverse set of 73 OLED materials. All descriptors were derived solely from the chemical structures of the organic compounds. A satisfactory average absolute error of 17.9 K for a test set of 15 OLED materials makes the model very useful for the prediction of the unknown OLED materials.

INTRODUCTION

Organic light-emitting-diodes (OLED) materials have attracted a great deal of attention, due to their promising applications in full-color, flat-panel displays as well as being a standpoint of scientific interest. Recently, pioneering work using the low molecular weight organic materials on electroluminescent (EL) devices has triggered extensive research and development of this field.[1] The organic molecular solids may form uniform, transparent amorphous thin film by vapor deposition or spin-coating methods. Compared with liquid crystal display, OLED displays possess wider view angle and faster response time. In contrast to polymers, they are pure materials with well-defined molecular structures and definite molecular weights without any distribution. The OLED materials should meet the following requirements: (1) suitable ionization potential and electron affinity so that the charge can be easily injected from the electrodes, (2) appropriate carrier mobility, not too high or too low, and (3) thermally stable and so on.[2] With respect to the thermal stability, the glass transition temperature T_g is the most important factor for the low molecular-weight amorphous molecular materials. The T_g of amorphous molecules is understood as the temperature at which a group of molecules start to move due to the intramolecular bond rotations. It leads to changes in the refractive index of molecules, the thermal expansion, and the heat capacity. To achieve stable OLED devices, molecular materials with high T_g are desirable.

Usually the T_g values for the molecular materials are measured by differential scanning calorimetry (DSC). However, different measurements can give different results, which strongly depend on whichever point has been selected in the

DSC curve.[4,7,12] For example, in the measurements of T_g for BNpA-1T,[7] the T_g values can be taken as 360, 364, or 369 K, corresponding to the onset point, the middle point, or the end point, respectively, in the DSC curve for the glass transition process. In addition, the obtained T_g values are strongly affected by the heating rate and other factors in the DSC measurement.[18] In one word, the T_g values are difficult to be determined experimentally because the transition takes place over a comparatively wide range of temperature.

An alternative approach to estimate T_g is quantitative structure−property relationship (QSPR). The QSPR has become a powerful theoretical tool for the descriptor and prediction of properties of complex molecular systems in different environments. The QSPR has been successfully applied to predict the chemical, physical, biochemical, and pharmacological properties of compounds; however, there have been relatively few attempts to correlate and predict T_g[3] of OLED materials. The object of the present work is to develop a QSPR model for T_g, which is expected to predict T_g of OLED materials and to help to understand the physical mechanisms determining the T_g of OLED materials. Katritzky et al. have developed a powerful QSPR program, the CODESSA (Comprehensive Descriptors for Structural and Statistical Analysis) package, which has been successfully used in many fields. In this work, we investigate a group of 88 organic materials, all of which are OLED materials. We first optimized these molecular structures, then calculated all kinds of descriptors by CODESSA. And then through the best multilinear regression method (BMLR), we obtained a six-parameter-correlation equation, which can be applied to predict the T_g values of the OLED materials.
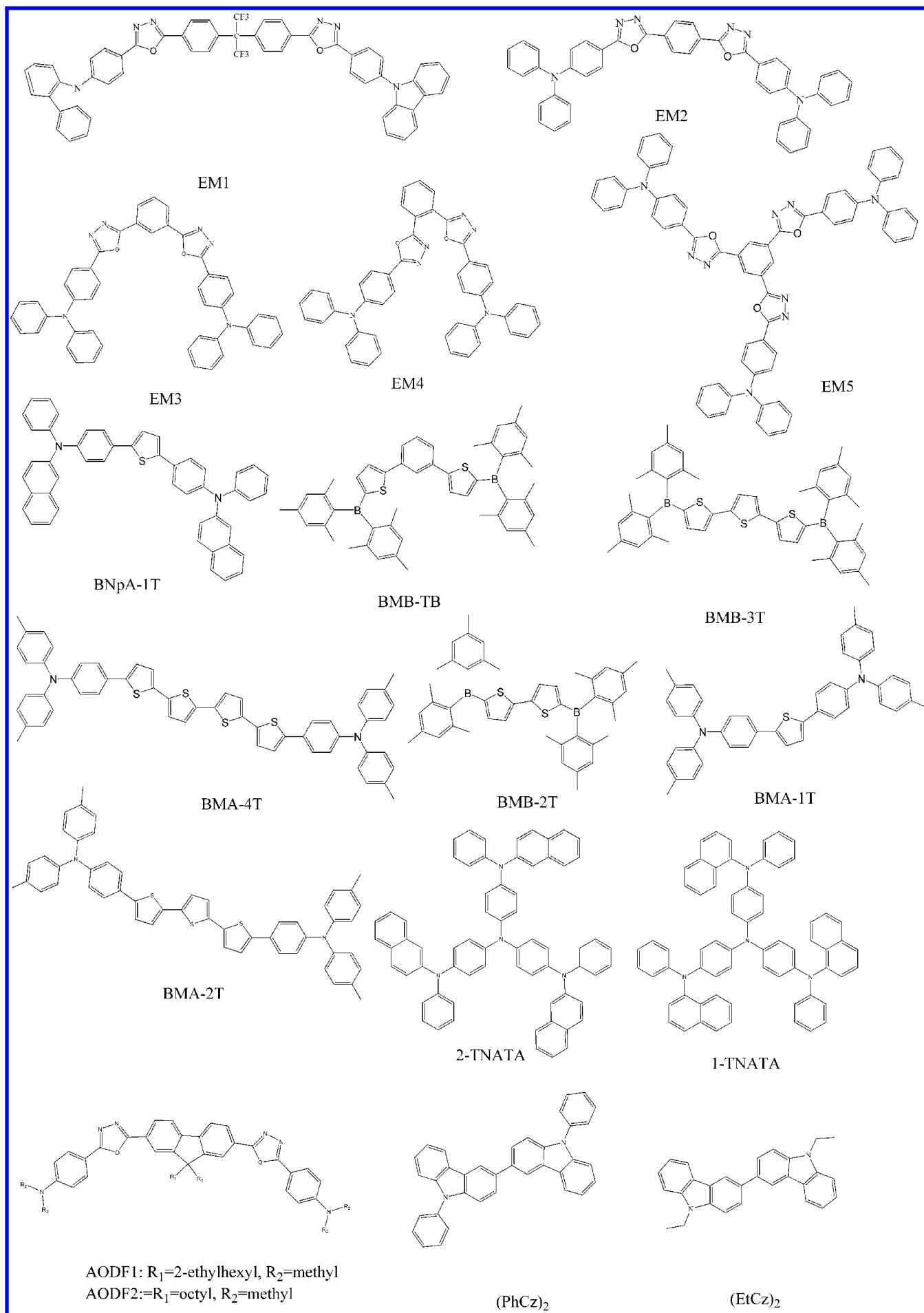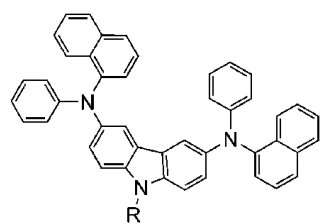
METHODOLOGY

Database Construction. The molecular structures of the 88 organic materials are depicted in Figure 1. These

---

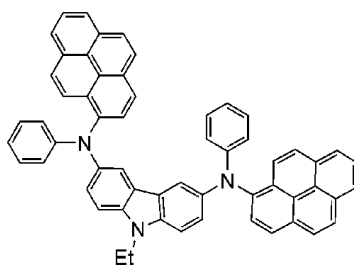* Corresponding author e-mail: zgshuai@iccas.ac.cn.
[†] Laboratory of Organic Solids.
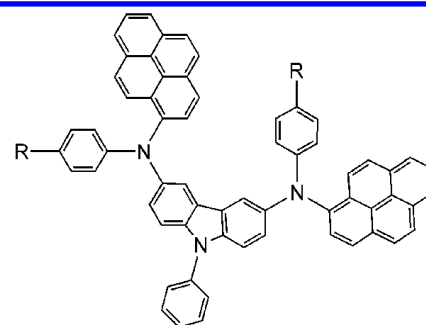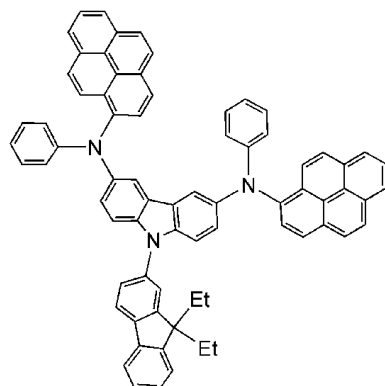[‡] Laboratory of Colloid and Interface Sciences.

EM1

EM2

EM3

EM4

EM5

BNpA-1T

BMB-TB

BMB-3T

BMA-4T

BMB-2T

BMA-1T

BMA-2T

2-TNATA

1-TNATA

AODF1: R₁=2-ethylhexyl, R₂=methyl
AODF2:=R₁=octyl, R₂=methyl
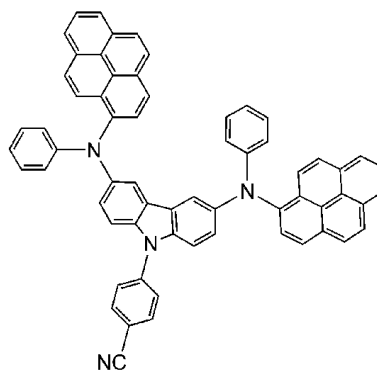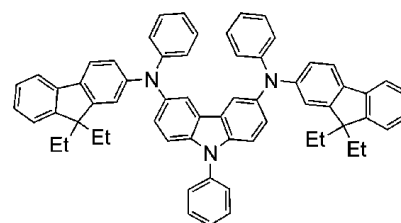
(PhCz)₂

(EtCz)₂

ENPCA:R=Et, NPCA:R=Ph

EPPCA

PPCA:R=H, PPPCA:R=Me, MPPPCA:R=OMe

EFPPCA
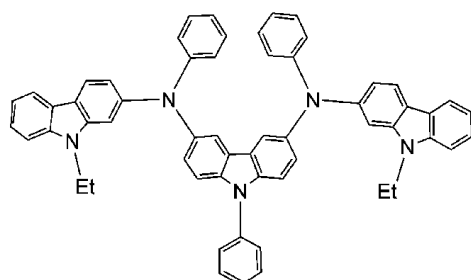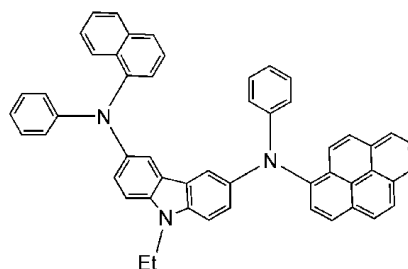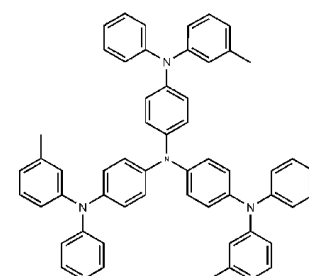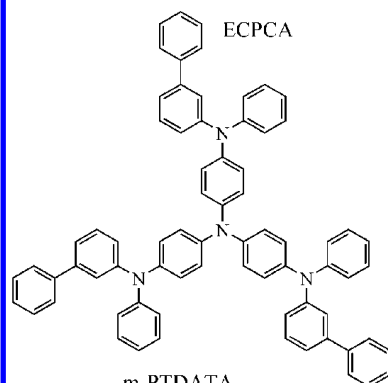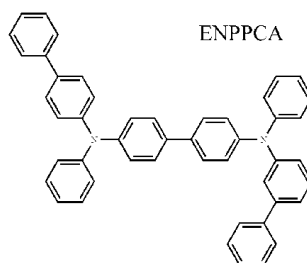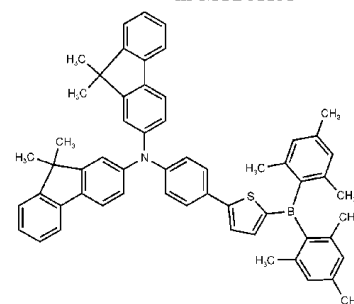
PPACBN

EFPCA

ECPCA

ENPPCA

m-MTDATA

m-PTDATA

m-BPD

F1AMB-1T

MTBDAB

PATB4e

PAPA

GLASS TRANSITION TEMPERATURE OF OLED MATERIALS

J. Chem. Inf. Comput. Sci., Vol. 43, No. 3, 2003 **973**
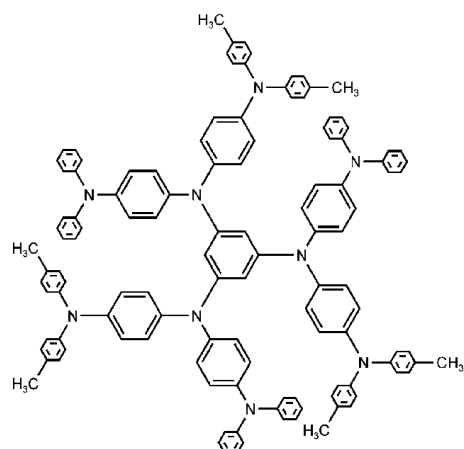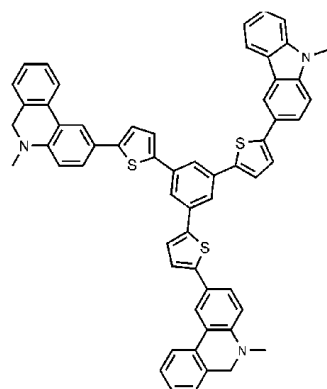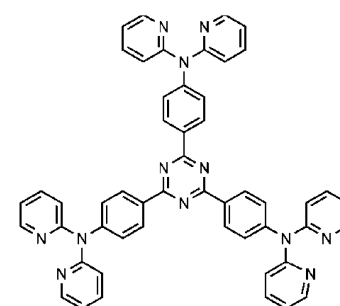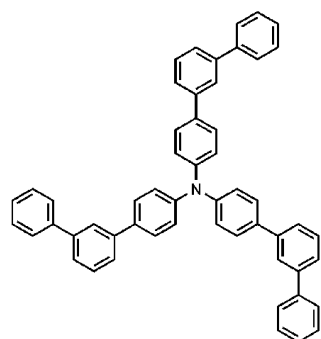
m-TTA
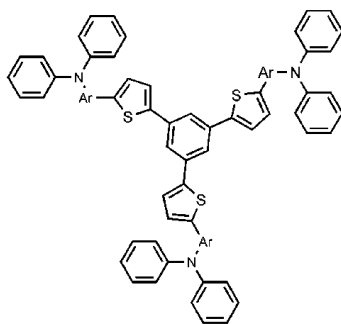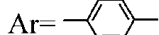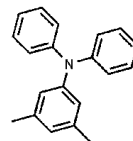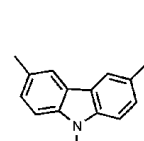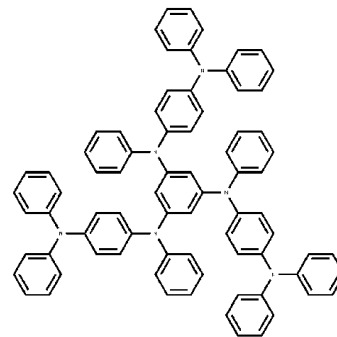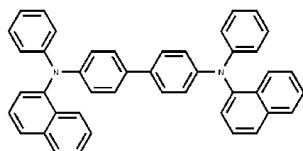
NPB
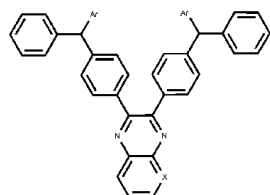
NPNAPQ:X=CH,Ar=1-Naphthyl   NPEFAPPP:X=N,Ar=9,9-diethyl-2-fluorenyl
NPNPPP :X=N,Ar=1-Naphthyl   NPECAPQ:X=CH,Ar=9-ethyl--3-carbazolyl
NEFAPQ: X=CH,Ar=9,9-diethyl-2-fluorenyl   NPECAPPP:X=N,Ar=carbazolyl

PATB4a-d:

Ar=

4a   4b   4c   4d

PAE3b-ef°

R=

3b   3c   3d   3e

p-DPA-TDAB
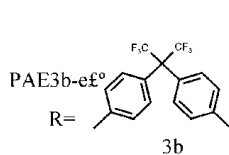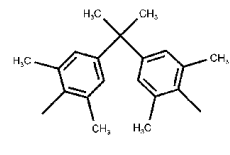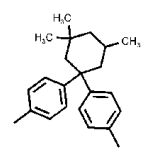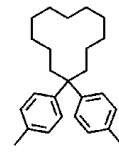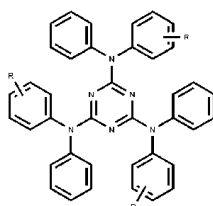
o-MTDATz:R=o-Me; m-MTDATz :R=m-Me
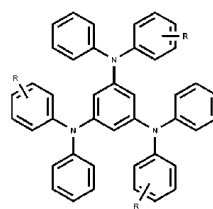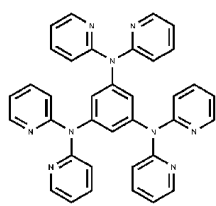
PAB   o-MTDAB:R=o-Me; m-MTDAB:R=m-Me;
p-MTDAB:R=p-Me
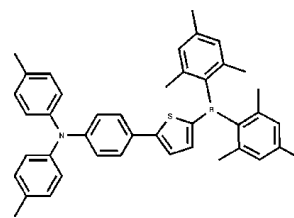
PhAMB-1T
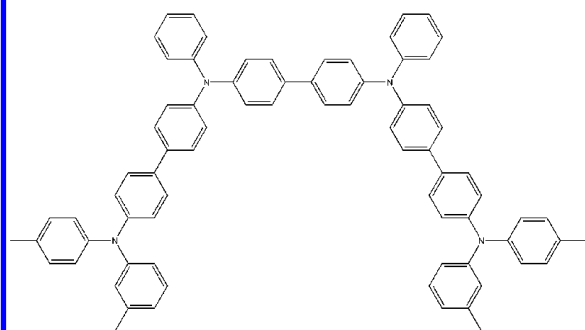
TPTE
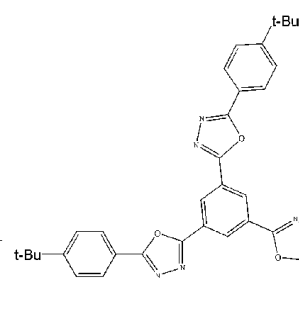
TPOB
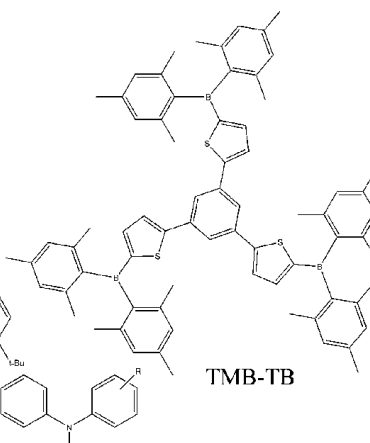
TMB-TB
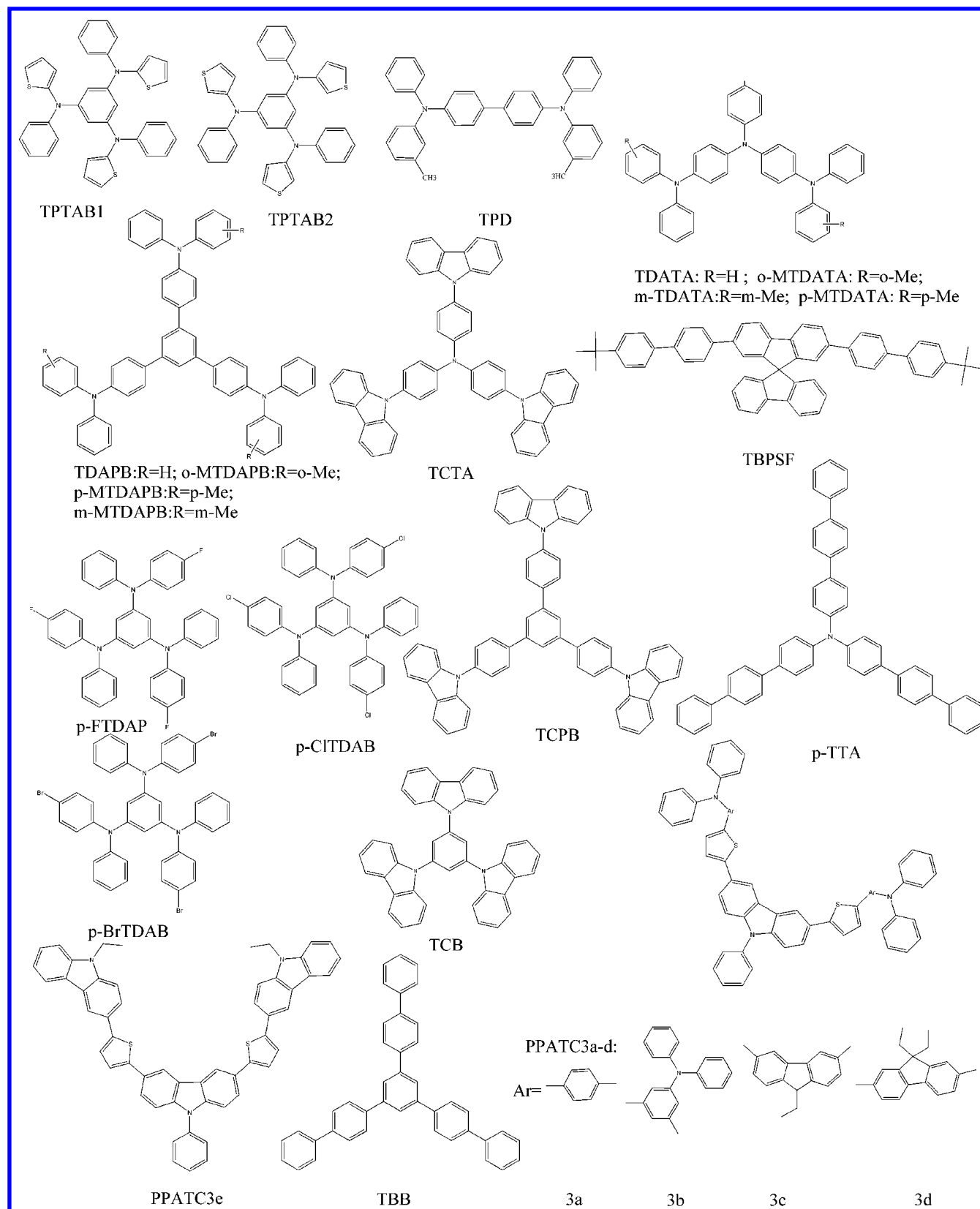
Figure 1. The compounds' structures included in the training and the prediction set.

molecules are used for our QSPR study, namely, the relationship between molecular structures and T_g. All the compounds are OLED materials, among which, 73 compounds are randomly chosen as the training set, and the other 15 compounds were used as the test set. The experimental T_g values were taken from literature.[3-14] The T_g values of

the data set span between 311 and 468 K, see Tables 1 and 3.

Molecular Descriptors. The molecular geometries were optimized by the semiempirical quantum chemical method AM1 (Austin Model 1) programs. The optimum molecular structures were used to calculate the energy and related

Table 1. Compounds Studied in Training Set with Observed and Calculated $T_g(K)$ Values

structure	calcd T_g	exptl T_g	diff	structure	calcd T_g	exptl T_g	diff
(PhCz)2[3]	384.4	363	21.4	TCTA[14]	412.2	423	−10.8
PAB[4]	408.4	401	7.4	TDATA[14]	349.4	362	−12.6
PATB4a[13]	402.0	398	4.0	TMB−TB[8]	425.6	433	−7.4
PATB4b[13]	426.1	415	11.1	TPD[3]	330.1	338	−7.9
PATB4c[13]	448.9	449	−0.1	TPOB[14]	395.2	410	−14.8
PATB4d[13]	429.9	423	6.9	TPTAB1[14]	315.5	311	4.5
PATB4e[13]	422.9	416	6.9	TPTAB2[14]	330.4	319	11.4
1−TNATA[3]	400.6	386	14.6	TPTE[3]	399.5	403	−3.5
PAPA[4]	400.2	394	6.2	BMA−2T[14]	378.8	363	15.8
2−TNATA[3]	397.7	383	14.7	BMA−3T[14]	371.2	366	5.2
PPATC3a[13]	400.7	401	−0.3	BMB-3T[14]	375.3	388	−12.7
PPATC3b[13]	417.3	419	−1.7	EMI[3]	399.7	407	−7.3
PPATC3c[13]	432.9	449	−16.1	EM3[3]	394.6	391	3.6
PPATC3d[13]	435.0	429	6.0	EM4[3]	377.7	372	5.7
PPATC3e[13]	417.1	415	2.1	EM5[3]	432.7	440	−7.3
AODF1[3]	362.4	353	9.4	F1AMB−1T[10]	407.6	397	10.6
AODF2[3]	364.0	353	11.0	m−BPD[14]	365.1	354	11.1
BMA−1T[14]	354.0	359	-5.0	m−PTDATA[14]	381.4	364	17.4
BMA−4T[14]	382.8	371	11.8	PhAMB−1T[10]	350.7	357	−6.3
BMB−TB[8]	382.2	382	0.2	m−MTDAB[14]	321.2	320	1.2
BNpA−1T[7]	368.4	364	4.4	m−MTDAPB[14]	372.8	378	−5.2
PAE3b[3]	386.5	388	−1.5	m−MTDATA[14]	351.8	348	3.8
PAE3c[3]	399.0	412	−13.0	NPECAPPP[6]	413.7	425	−11.3
PAE3d[3]	392.8	406	−13.2	NPECAPQ[6]	404.4	415	−10.6
NPCA[11]	393.2	396	−2.8	NPNAPQ[6]	403.4	387	16.4
EPPCA[11]	447.0	447	0.0	NPNPPP[6]	413.0	400	13.0
PPCA[11]	454.1	453	1.1	o−MTDAB[14]	324.9	315	9.9
PPACBN[11]	479.9	467	12.9	o−MTDAPB[14]	381.2	382	−0.8
EFPCA[11]	404.0	405	−1.0	o−MTDATA[14]	357.8	349	8.8
ENPPCA[11]	421.7	447	−25.3	o−MTDATz[14]	325.5	328	-2.5
PPPCA[11]	455.7	457	−1.3	p−BrTDAB[14]	328.6	345	-16.4
ENPCA[11]	383.9	393	−9.1	p−ClTDAB[14]	327.0	337	-10.0
TBB[9]	357.0	361	−4.0	p−DPA−TDAB[14]	387.0	380	7.0
TCB[14]	392.4	399	−6.6	p−FTDAB[14]	329.0	327	2.0
TCPB[14]	418.0	445	−27.0	p−MTDAB[14]	318.6	328	−9.4
p−MTDATA[14]	358.4	353	5.4	p−MTDAPB[14]	378.2	383	−4.8
p−TTA[14]	389.7	405	−15.3				

Table 2. Descriptor Involved in the Best Six-Parameter QSPR Model Derived for T_g [a]

descriptor	X	DX	*t*-test
intercept	−23093	1898.3	−12.165
RNR	1755.1	79.482	22.082
I_B	−11325	2887.3	−3.9225
PPSA-2/TMSA	112.69	9.3925	11.998
AVCA	5843.5	476.07	12.274
HASA−1	0.40511	0.050715	7.9880
THC	142.20	23.552	6.0377

[a] $R^2 = 0.9270$, $F = 139.61$, $s^2 = 114.97$, $R^2_{cv} = 0.9105$.

properties by the AM1 programs. Then the output files were used for producing constitutional, topological, electrostatic, geometrical, quantum-chemical, and thermodynamic descriptors by CODESSA software package. The resulting descriptors were then used for multilinear scale treatment.

Determination of Optimum Descriptors Set. We use the heuristic method and the best multilinear regression method (BMLR), as implemented in CODESSA package, to search for the set of best multilinear correlation. In the case of the heuristic method, the descriptors are ordered by decreasing correlation coefficient when one-parameter regression is used. The next step involves correlation of the given property with the top descriptor in the above list with each of the remaining descriptors and the next one with each of the remaining descriptors, etc. The best pairs, as evidenced by the highest *F*-values in the two-parameter correlations, are chosen and used for further inclusion of descriptors in a similar manner.

The BMLR method searches for the multiparameter regression with the maximum predicting ability using the following strategy:

1. All the orthogonal pairs of descriptors *i* and *j* (with $R^2_{ij} < 0.1$) are found in a given data set. The pairs with highest regression correlation coefficient R^2 with the property are chosen for performing the higher order treatments.

2. For each descriptor pair obtained, a noncollinear descriptor scale *k* (with $R^2_{ik} < 0.6$, $R^2_{jk} < 0.6$) is added, and the respective three-parameter regression treatment is performed. The descriptor triples with the highest R^2 are chosen for the next step.

3. For each descriptor set, chosen in the previous step, an additional noncollinear descriptor scale is added, and the respective $(n+1)$-parameter regression treatment is performed.

4. The final result is obtained when the increase in R^2 is below a given threshold value. Otherwise step 4 is repeated.

RESULTS AND DISCUSSION

The number of descriptors in the final QSPR was determined on the basis of the obtained correlation coefficient, Fisher criterion, and cross-validated correlation coefficient as well as the rationality of the chosen descriptors with respect to the glass transition process. In short, the QSPR model is most appropriate if the correlation coefficient, the Fisher criterion, and the cross-validated correlation coefficient are high, namely, the descriptors can reasonably

Table 3. Compounds Studied in Test Set with Observed and Calculated $T_g(K)$ Values

structure	calcd T_g	exptl T_g	diff	structure	calcd T_g	exptl T_g	diff
(EtCz)2[3]	342.3	343	−0.7	TBPSF[5]	440.0	468	−28.0
BMB-2T[9]	366.6	380	−13.4	TDAPB[14]	371.1	394	−22.9
BPAPF[12]	419.1	440	−20.9	EFPPCA[11]	463.7	458	5.7
PAE3e[3]	387.5	417	−29.5	MPPPCA[11]	451.1	456	−4.9
EM2[3]	389.9	395	−5.1	m−MTDATz[14]	318.2	315	3.2
MTBDAB[14]	414.0	407	7.0	NEFAPQ[6]	421.4	389	32.4
NPB[3]	382.5	368	14.5	NPEFAPPP[6]	439.8	395	44.8
M−TTA[14]	388.1	353	35.1				

explain the glass transition process. In this way, the best six-parameter correlation equation is obtained from the training set of 73 compounds, which has the squared correlation coefficient $R^2 = 0.9270$ and a cross-validated correlation coefficient $R^2_{cv} = 0.9105$ as detailed in Tables 1 and 2.

The best six-parameter correlation equation is the following:

$$T_g = 1755.1\text{RNR} - 11325I_B + 112.69\text{PPSA} -$$
$$2/\text{TMSA} + 5843.5\text{AVCA} + 0.40511\text{HASA-1} +$$
$$142.20\text{THC}-23093 \quad (1)$$

Here RNR is the relative number of rings; I_B is the principal moment of inertia of axis-B; PPSA-2/TMSA is the fractional of the total charge weighted partial positive surface area (PPSA-2) and the total molecular surface area (TMSA); AVCA is the average valence of a C atom; HASA-1 is H-acceptors surface area [Zefirov's PC]; and THC is the total heat capacity (at 300 K) over the total number of atoms.

The first important descriptor is the relative number of rings (RNR), namely the constitutional descriptor, accounts for the chain stiffness of small molecules. The principal moment of inertia I_B is equal to $\sum_i m_i r_{iy}^2$, where m_i is the mass of atom i and r_{iy} denotes the distance of the ith atom from the main rotational axes y of the molecule.[15] The principal moment of inertia I_B, the geometrical descriptor, shows both the rigid rotator approximation and the mass distribution in the molecule. The average valence of a C atom, the quantum-chemical descriptor, may indirectly descriptor the flexible degree of the molecule. The electrostatic descriptors PPSA-2/TMSA and HASA-1 account for intermolecule electrostatic interaction force. The total heat capacity (at 300 K) over a number of atoms, the thermodynamic descriptor, is calculated in terms of the vibrational motions of its atoms; therefore, it accounts for all the possible modes of motion of atoms or groups of atoms in a molecule. Such motions include bond stretching, bond bending and "rocking" motions, torsional oscillations, the "flipping" of a structural unit from one equilibrium position to another, and large-scale cooperative motions.[18] These descriptors indicate the importance of the chain stiffness and rigid electrostatic field as well as vibrational motions effect on the T_gs of the small molecules.

Using eq 1, we can predict the T_g values of the 15 compounds in the test set, which are listed in Table 3. From Tables 1 and 3, the average errors of the training set and the test set are 8.5 and 17.9 K, respectively. Several investigations have been carried out in applying QSPR to establish the statistical model for T_g in polymeric materials.[16,17] Katritzky et al. have studied the glass transition temperatures in polymeric materials using QSPR by the CODESSA

package. They developed a different approach which, using the molar T_g ($T_g/M_{repeat,unit}$) instead of T_g as the dependent variable they produced a five-parameter correlation ($R^2 = 0.946$) for 88 polymers training set. However, if they use the T_g values as the dependent variable, they produces a model with a correlation coefficient $R^2 = 0.830$. From their model, the most significant descriptor is the moment of inertia (I_C), which is the same as the I_B in our correlation. Recently, Mattioni et al.[19] have applied both monomer and repeat unit structures to develop QSPR models for T_gs of the polymers. Only topological descriptors were calculated. Using computational neural networks (CNNs), they have produced a model with rms error of 10.1 K ($R^2 = 0.98$) for 165 polymers. The most significant descriptor, the atom valence-corrected third-order kappa index (KAPA-6), encodes information about the size and branching of molecule. It has similar physical meaning as the RNR and I_B in our model. However, with multiple linear regression analysis (MLRA) method, they produced a 10-descriptor MLRA model with rms error of 40.06K ($R^2 = 0.846$) for 131 polymers training set. Meanwhile, Kim et al.[3] obtained a seven-parameter QSPR model with correlation coefficient ($R^2 = 0.989$) for T_gs of small molecules by Genetic Algorithm (GA) and multilinear regression. The most significant factor is the number of bonds in a molecule (SC-1). In fact, their factor SC-1 is related to the rotational motion and has a very similar physical meaning as the I_B and RNR. In their model, only 16 electroluminescent molecules, out of 81 molecules in total, are kept in the training set. From models we have mentioned above, we find that the essential characters of their most significant descriptors have been kept in our model. In our system, the constitutional, topological, electrostatic, geometrical, quantum-chemical, and thermodynamic descriptors of OLEDs materials were applied to develop our QSPR model. In addition, as we know, the T_g values of amorphous materials themselves are very difficult to determine experimentally, our predictions are reasonable.

The present six-parameter correlation equation can be applied to predict the T_g values of the small molecules used in organic electroluminescent devices. Compared with the group additive method,[18] this six-parameter QSPR of the T_gs of OLED materials can predict the unknown and unavailable compounds which have similar structures with training set compounds.

CONCLUSION

To summarize, we correlated the glass transition temperature T_g with the molecular structure for the OLEDs molecules containing different substituents. We obtained a six-parameter correlation equation, which can be applied to predict the T_g of OLEDs materials. The geometrical descrip-
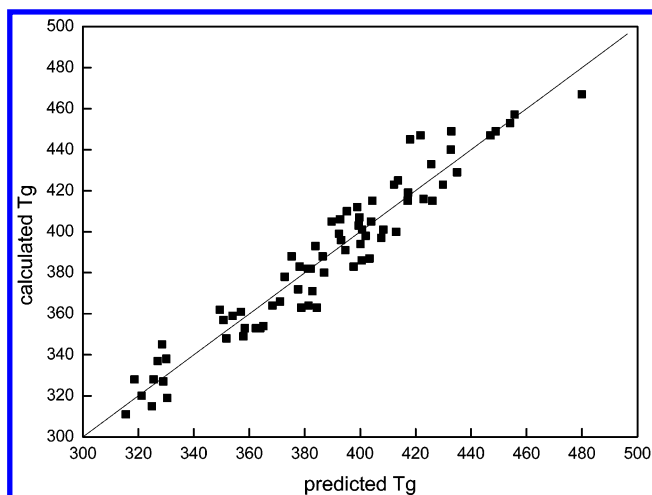
GLASS TRANSITION TEMPERATURE OF OLED MATERIALS

J. Chem. Inf. Comput. Sci., Vol. 43, No. 3, 2003 **977**

Figure 2. Plot of calculated versus experimental values of T_g for 73 OLED materials.

tor (I_B), constitutional descriptor (RNR), electrostatic descriptors (PPSA-2/TMSA, HASA-1), quantum-chemical descriptor (AVCA), and thermodynamic descriptor (THC) are obtained by the CODESSA program which reflect directly the chain stiffness, rigid electrostatic field as well as vibrational motions effect on the T_gs, respectively. As the T_g of the amorphous materials are defined, these descriptors indeed reflect the microscopic origin of the glass transition temperature.

REFERENCES AND NOTES

(1) Tang, C. W.; Van Slyke, S. A. Organic electroluminescent diodes. *Appl. Phys. Lett.* **1987**, *51*, 913−915.
(2) Tang, C. W.; Van Slyke, S. A.; Chen, C. H. Electroluminescence of doped organic thin films. *J. Appl. Phys.* **1989**, *65*, 3610−3616.
(3) Kim, Y. S.; Kim, J. H.; Kim, J. S.; No, K. T. Prediction of glass transition temperature (*T*g) of some compounds in organic electroluminescent devices with their molecular properties. *J. Chem. Inf. Comput. Sci.* **2002**, *42*, 75−81.
(4) Pang, J.; Tao, Y.; Freiberg, S.; Yang, X. P.; D'Iorio, M.; Wang, S. Syntheses, structures, and electroluminescence of new blue luminescent star-shaped compounds based on 1,3,5-triazine and 1,3,5-trisubstituted benzene. *J. Mater. Chem.* **2002**, *12*, 206−212.
(5) Wu, C. C.; Lin, Y. T.; Chiang, H. H.; Cho, T. Y.; Chen, C. W.; Wong, K. T.; Liao, Y. L.; Lee, G. H.; Peng S. M. Highly bright blue organic light-emitting devices using spirobifluorenecored conjugated compounds. *Appl. Phys. Lett.* **2002**, *81*(4), 577−579.
(6) Thomas, K. R. J.; Lin, J. T.; Tao, Y. T.; Chuen, C. H. Quinoxalines incorporating triarylamines: potential electroluminescent materials with tunable emission characteristics. *Chem. Mater.* **2002**, *14*, 2796−2802.
(7) Liu, P.; Tong, Z. Anovel greenish blue-emitting amorphous molecular material: 2,5-bis{4-[2-naphthyl(phenyl)amino]phenyl}thiophene. *Chinese J. Chem.* **2001**, *19*, 979−982.
(8) Kinoshita, M.; Shirota, Y. 1,3-Bis[5-(dimestylborryl)thiophen-2-yl]-benzene and 1,3,5-tris[5-(dimesityl-boryl) thiophen-2-yl] benzene as a novel family of electron-transporting hole blockers for organic electroluminescent devices. *Chem. Lett.* **2001**, (7), 614−615.
(9) Noda, T.; Ogawa, H.; Shirota, Y. A blue-emitting organic electroluminescent device using a novel emitting amorphous molecular material, 5, 5′-bis(dimesitylborryl)-2,2 ′-bithiophene. *Adv. Mater.* **1999**, *11*(4), 283−285.
(10) Shirota, Y.; Kinoshita, M.; Noda, T. et al. A novel class of emitting amorphous molecular materials as bipolar radical formants: 2-{4-[bis-(4-methylphenyl)amino]phenyl}-5-(dimesitylborryl)thiophene and 2-(4-[bis(9,9-dimethylfluorenyl)amino]phenyl)-5-(dimesitylborryl)thiophene. *J. Am. Chem. Soc.* **2000**, *122*(44), 11021−11022.
(11) Thomas, K. R. J.; Lin, J. T.; Tao, Y. T.; et al. Light-emitting carbazole derivatives: Potential electroluminescent materials. *J. Am. Chem. Soc.* **2001**, *123*(38), 9404−9411.
(12) Ko, C. W.; Tao, Y. T. 9,9-bis{4-[di-(p-biphenyl)aminophenyl]fluorene: a high T−g and efficient hole-transporting material for electroluminescent devices. *Synthetic Metal* **2002**, *126*(1), 37−41.
(13) Thomas, K. R. J.; Lin, J. T.; Tao, Y. T.; et al. New star-shaped luminescent triarylamines: Synthesis, thermal, photophysical, and electroluminescent characteristics. *Chem. Mater.* **2002**, *14*(3), 1354−1361.
(14) Shirota, Y. Organic materials for electronic and optoelectronic devices. *J. Mater. Chem.* **2000**, *10*(1), 1−25.
(15) Katritzky, A. R.; Rachwal, P.; Law, K. W.; Karelson M. *CODESSA, Reference Manual*; Semichem and University of Florida: 1995−1997.
(16) Katritzky, A. R.; Rachwal, P.; Law, K. W.; Karelson M.; Lobanov, V. S. Prediction of polymer glass transition temperatures using a general quantitative structure−property relationship treatment. *J. Chem. Inf. Comput. Sci.* **1996**, *36*, 879−884.
(17) Katritzky, A. R.; Sild, S.; Lobanov, V.; Karelson, M. Quantitative structure−property relationship (QSPR) correlation of glass transition temperatures of molecular weight polymers. *J. Chem. Inf. Comput. Sci.* **1998**, *38*, 300−304.
(18) Bicerano J. *Prediction of Polymer Properties*, 3rd ed.; Marcel Dekker, Inc.: New York, 1996.
(19) Mattioni B. E.; Jurs P. C. Prediction of Glass transition Temperatures from Monomer and repeat unit structure Using Computational Neural Networks. *J. Chem. Inf. Comput. Sci.* **2002**, *42*, 232−240.

CI034011Y